Research Journal of Applied Sciences, Engineering and Technology 6(7): 1227-1232, 2013
DOI:10.19026/rjaset.6.3936
ISSN: 2040-7459; e-ISSN: 2040-7467
© 2013 Maxwell Scientific Publication Corp.
Submitted: September 30, 2012 Accepted: December 02, 2012 Published: July 05, 2013

Research Article

Denoising Process on Body Vibration Signals from Caterpillar Nodule Collector on the Soft Quality Bottom of the Sea

[1, 2]Zeng Yi-hui, [2]Zhou Yucai, [1]Liou Dao-cai and [3]Zuo Qing-song
[1]Anhui Wonder University of Information Engineering, Hefei 231201, Anhui, China
[2]College of Mechanical and Electrical Engineering of Central South University, Changsha 410083, Hunan, China
[3]College of Mechanical and Vehicle Engineering, Hunan University, Changsha 410082, Hunan, China

Abstract: Regarding the diversity and complexity of the road conditions on the soft sediment seabed, in order to improve the driving control precision of the caterpillar nodule collector, this study, focusing on the noise disturbance of the nodule collector body, adopts the methods of wavelet packet decomposition algorithm and Hilbert-Huang transformation algorithm to reconstruct the nodule collector body vibration signals, which are targeted by Hilber-Huang transformation algorithm to reach IMF fraction in the process of Empirical Mode Decomposition. Therefore, through the Hilbert spectrum analysis of IMF component, IMF component power characteristics are achieved, the available IMF component is optioned to reconstruct signals and the disturbance of the noise is eliminated. Comparing to the approach of wavelet decomposition, Hilbert-Huang transformation's analysis and algorithm of the collector body's vibration signals' reconstruction are more accurate, providing valid control parameter to control the drive of caterpillar nodule collector on the soft quality bottom of the sea more precisely.

Keywords: Empirical mode decomposition, hibert spectrum, hilber-huang changes, IMF component, nodule collector's body vibration signals, wavelet decomposition

INTRODUCTION

In the deep-sea mining system, caterpillar nodule collector is applied to collect polymetallic nodule, which, during its operation, is affected by coincident and complicated environmental factors, including wind, wave, sea current and submarine high-voltage, etc. Its performance in the fields of kinematics and dynamics is complex enough to bring immense challenge to the control system of the caterpillar nodule collector that runs on the soft sediment (Dai and Shao-Jun, 2009; Wang and Liu, 2004; Liu *et al*., 2003).

In the control system, the collected collector's vibration signals are unavoidably interrupted by noise. Furthermore, as the measured signals and the disturbing signals are non-stationary signals, it is a tough job to eliminate the noise by adopting the filtering method. For example, while using Fourier filtering method to filter the noise (Alsdorf, 1997), Gaussian noise as well as some important high-frequency information is destroyed; while using spline fitting method (Xian-Liang *et al*., 1996), though Gaussian noise is perfectly ceased, some invalid information will enter the control system.

This study mainly aims to apply the approaches of wavelet decomposition and Hilbert-Huang changes (Wei *et al*., 2010; Rai and Mohanty, 2007; Li *et al*., 2008; Dong *et al*., 2008a, b) to deal with crawler-style set tub's vibration signals, in the meantime, those respectively received reconstructed signals and the practical vibration signals are compared and contrasted. It is shown that reconstructed vibration signals with Hilbert-Huang changes are more accurate.

This study, concentrating on the significant importance of the accuracy of control system which ensures the possibility of the caterpillar nodule collector's on the soft quality bottom of the sea, has great academic value and perspective for wide application in construction.

INTRODUCTON OF WAVELET DECOMPOSITION THEORY

Wavelet packet: Consider Orthogonal wavelet basis's Filter coefficients as h (n) and g (n) respectively, in addition that criterion function φ (t) is changed into ω_0 (t) and wavelet function ψ (t) into ω_1 (t). Then, two-scale equations about scale function φ (t) and wavelet function ψ (t) are:

Corresponding Author: Zeng Yi-hui, College of Mechanical and Electrical Engineering of Central South University, Changsha 410083, Hunan, China, Tel.: 15256003168
This work is licensed under a Creative Commons Attribution 4.0 International License (URL: http://creativecommons.org/licenses/by/4.0/).

$$\omega_0(t) = \sqrt{2}\sum_{n\in Z} h(n)\omega_0(2t-n) \quad (1)$$

$$\omega_1(t) = \sqrt{2}\sum_{n\in Z} g(n)\omega_0(2t-n) \quad (2)$$

H (ω) and G (ω) are the Fourier transformation for h (n) and g (n) respectively:

$$H(\omega) = \frac{1}{\sqrt{2}}\sum_{n\in Z} h(n)e^{jn\omega} \quad (3)$$

$$G(\omega) = \frac{1}{\sqrt{2}}\sum_{n\in Z} g(n)e^{jn\omega} \quad (4)$$

Fourier transformation for two-scale equations is:

$$W_0(\omega) = H(\omega)W_0(\omega/2) \quad (5)$$

$$W_1(\omega) = G(\omega)W_0(\omega/2) \quad (6)$$

A new space U^l_j is proposed as a united representation for scale space V_j and a wavelet Space W_j. Suppose that:

$$\begin{cases} U_j^0 = V_j \\ U_j^1 = W_j \end{cases} \quad (7)$$

Hence, multiple resolving power space's orthogonal decomposition $V_{j-1} = V_j \oplus W_j$ is able to be united by U^I_j's decomposition:

$$U^0_{j-1} = U^0_j \oplus U^1_j \quad (8)$$

It is to define subspace U^l_j to be function ω_l (t)'s closure space, but U^{2l}_j is function ω_{2l} (t)'s closure space. Then ω_l (t) is fit to the following two-scale equations:

$$\omega_{2l}(t) = \sqrt{2}\sum_{n\in Z} h(n)\omega_l(2t-n) \quad (9)$$

$$\omega_{2l-1}(t) = \sqrt{2}\sum_{n\in Z} g(n)\omega_l(2t-n) \quad (10)$$

And,

$$U^l_{j-1} = U^{2l}_j \oplus U^{2l+1}_j \quad (11)$$

Wavelet packet $\{\omega_l$ (t)$\}$ is defined as a correspondent function set, including scale function ω_0 (t) = φ (t) and wavelet function ω_1 (t) = ψ (t).

Wavelet packet decomposition: Suppose l = 1, 2,…, n and j = 1, 2,…, n. The Eq. (11) is decomposed iteratively as follows:

$$U^1_j = W_j = U^2_{j+1} \oplus U^3_{j+1} \quad (12)$$

However,

$$U^2_{j+1} = U^4_{j+2} \oplus U^5_{j+2}, \quad U^3_{j+1} = U^6_{j+2} \oplus U^7_{j+2} \\ \vdots \quad (13)$$

Therefore, various decompositions from wavelet space W_j can be achieved:

$$\begin{aligned} W_j &= U^2_{j+1} \oplus U^3_{j+1} \\ W_j &= U^4_{j+2} \oplus U^5_{j+2} \oplus U^6_{j+2} \oplus U^7_{j+2} \\ &\vdots \\ W_j &= U^{2^l}_{j+2} \oplus U^{2^l+1}_{j+2} \oplus \cdots \oplus U^{2^{l+1}+1}_{j+2} \\ &\vdots \end{aligned} \quad (14)$$

The decomposed subspace sequence from W_j space can be rewritten into U^{2l+m}_{j+l}, m = 0, 1,…, 2l-1; l = 1, 2, …, j; j = 1, 2, …. Subspace sequence U^{2l+m}_{j+l}'s standard orthonormal basis is:

$$\{2^{-(j+l)/2}\omega_{2^l+m}(2^{-(j+l)}t-n), \quad n\in Z\} \quad (15)$$

When l = 0 and m = 0, subspace sequence U^{2l+m}_{j+l} is abbreviated to be $U^l_j = W_j$, the correlated orthonormal basis to be $\{2^{-j/2} w_1 (2^{-j}$ t-n) = $2^{-j/2}$ ψ (2^{-j} t-n)$\}$, which is right to be standard orthonormal wavelet basis {ψj, n (t)}.

INTRODUCTION OF HIBERT-HUANG CHANGES

The basic idea of EMD decomposition (Loutridis, 2004; Chang and Lee, 2009; Jia-Qiang *et al*., 2008):

- Find signals' all local minimums and use line transect three times to string all the local maximum points and local minimum points to form upper and below envelope, which contain all the data points. The medium value of two envelop lines are marked as m_1, the difference between X and m_1 is h_1:

$$h_1(t) = X(t) - m_1(t) \quad (16)$$

  If h_1 (t) satisfies IMF's condition, h_1 (t) is an IMF and h_1 (t) is the first component for X (t).
- If h_1 can't satisfy IMF's definition, h_1 (t) is considered as original data, the repetition of the former procedure leads to:

$$h_{11}(t) = h_1(t) - m_{11}(t) \tag{17}$$

where, m_{11} (t) is the average of the upper and lower envelope and then it's time to judge whether h_{11} (t) satisfies IMF's definition. In case that satisfaction fails, the loop will be repeated k times to reach an answer h_{1k} (t) = h_1 (k-1) (t) -m_{1k} (t), which is enough to enable m_{1k} (t) to satisfy IMF's definition with a mark $c_1 = h_{1k}$.

- The following result embodies by separating c_1 from data X:

$$r_1(t) = X(t) - c_1(t) \tag{18}$$

And then turn r_1 (t) into new original data and repeat the procedures above once and again. As a result, the second fraction c_2 is reached to satisfy IMF. The repeated loops come to:

$$r_{i-1}(t) - c_i(t) = r_i(t),\ i = 2, 3, 4, \cdots, n \tag{19}$$

In order to determine the signal processing is no longer with IMF, IMF component is generally taken to end the loop. Now that it's harsh to have IMF components satisfy condition (2), width wave is supposed to be deleted in a physical sense. For this reason, condition (2) should follow more valid quantity criterion to make sure that every IMF is in width and frequency's physical sense. The standard is provided owing to Eq. (5):

$$\mathrm{SD} = \sum_{k=0}^{T} \frac{[m_{1(k-1)}(t) - m_{1(k-1)}(t)]^2}{m_{1(k-1)}^2(t)} \tag{20}$$

where,

m_{1k} (t) : Medium envelop realized by algorithm of this looping of IMF components' extracting modules
m_1 (k-1) (t) : Medium envelop in the last loop
0, …, T : All the time points that medium envelop line contains

The ideal SD value should be between 0.2-0.3. Those two conditions above that satisfy IMF components not only lay foundations of the consequent Hibert changes, but also render every component meaningful in a physical sense.

Not until r_n (t) becomes a monotonic function that is impossible to be extracted to meet IMF components, the loop comes to an end. So the initial data is the sum of IMF components and the final remnant and expressed as follows:

$$X(t) = \sum_{i=1}^{n} c_i(t) + r_n(t) \tag{21}$$

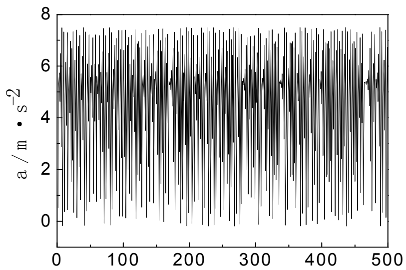

Fig. 1: Vibration signal including the noise about mining vehicle tracked body

Hilbert spectrum analysis of IMF components: Hilbert spectrum illustrates total vibration width (or power) distributed on every frequency value. It discovers the width (or power) accumulation on total data sequence so that power's distribution regularities in the scales of space (or time) are deliberately reflected during the physical process. And considering Hilbert changes of IMF components, IMF components' aggregate vibration width with correlated frequency is obvious on frequency spectrum. IMF components with minor power are regarded as noise and eliminated.

After Signal X (t) is decomposed into a number of IMF components by EMD treatment, Each IMF component c_i (t) through the Hilbert Transformation as follows:

$$H[c_i(t)] = \frac{1}{\pi}\int_{-\infty}^{+\infty} \frac{c_i(\tau)}{t-\tau} d\tau \tag{22}$$

When the Eq. (8), (9) and (10) are possible, the instantaneous envelop a_i (t) and frequency ω_i (t) will be reached:

$$a_i(t) = \sqrt{c_i^2(t) + H^2[c_i(t)]} \tag{23}$$

$$\varphi_i(t) = \arctan \frac{H[c_i(t)]}{c_i(t)} \tag{24}$$

$$\omega_i(t) = \frac{d\varphi_i(t)}{dt} \tag{25}$$

Original signal X (t) is the real component for Eq. (11) after Hilbert transformation of every IMF components.

NODULE COLLETOR'S BODY VIBRATION SIGNAL RECONTRUCTION

The collected signals in experiments were caterpillar nodule collector's body vibration signals when it runs on the soft quality bottom of the sea. In the first Fig. 1, there were 500 mixed signal data about collector's body vibration, including the noise.

Table 1: The band wavelet packet power percentage

Wavelet packet	Band power (%)
s (3, 0)	79.84
s (3, 1)	6.19
s (3, 2)	4.74
s (3, 3)	0.78
s (3, 4)	4.53
s (3, 5)	2.96
s (3, 6)	0.42
s (3, 7)	0.54

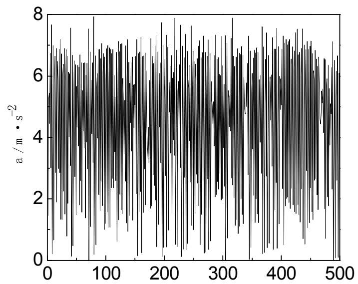

Fig. 2: Wavelet packet decomposition reconstruction of collector's body vibration signals

Wavelet decomposition reconstruction of collector's body vibration signals: Wavelet basis is a crucial element in wavelet transform. Reasonable option of wavelet means a lot to extract accurate signals and characteristics. Through the analysis of wavelet basis, it is known that Daubechies wavelet, Symlets wavelet and Coitlets wavelet are appropriate for vibration signal analysis of wavelet. Coiflets4 wavelet is chosen. Decompose signals with closure algorithm in K levels. In each process of decomposition, the nth frequency band of upper level j will be further divided into j+1's 2nth and 2n+1'Th frequency bands. Therefore, the frequency domain on k level will be divided into 0~fs/2k, fs/2k~2fs/2k,…, 2k-1 fs/2k~fs, among which fs has the highest frequency.

Based on the standard of coiflets4 wavelet packet, the decomposition of the signal in 3 levels will gain 8 wavelet packet in all, ranging from s (3, 0) ~s (3, 7) which are shown in the Table 1.

From the power characteristics of every frequency band and the percentage, wavelet packets s (3, 0), s (3, 1), s (3, 2), s (3, 4) with a wealth of wavelet packet feature information are regarded as distinctive wavelet packets, which are extracted and reconstructed and shown in Fig. 2.

Reconstruction of body vibration signals through hilbert-huang changes: Body vibration signals are decomposed and IMF components from IMF1 to IMF9 are obtained and shown in Fig. 3.

IMF1~IMF9 represent the gradually adaptive development from the low-level IMF components (the high-frequency elements are major in number) to the high-level IMF components (the low-frequency elements are major in number), through the process, the frequency components of the caterpillar nodule collector's body vibration signals will be extracted from high levels to low levels. Regarding EMD decomposition approach's internal characteristics, its basic function is adaptive in itself. Hence, without the influence of prior estimated basic function which ever greatly affected traditional signal analytic method, the achieved IMF1~IMF9 components are the real and direct responses to the signals. Figure 3 is IMF1~IMF9 components' Hilbert spectrum.

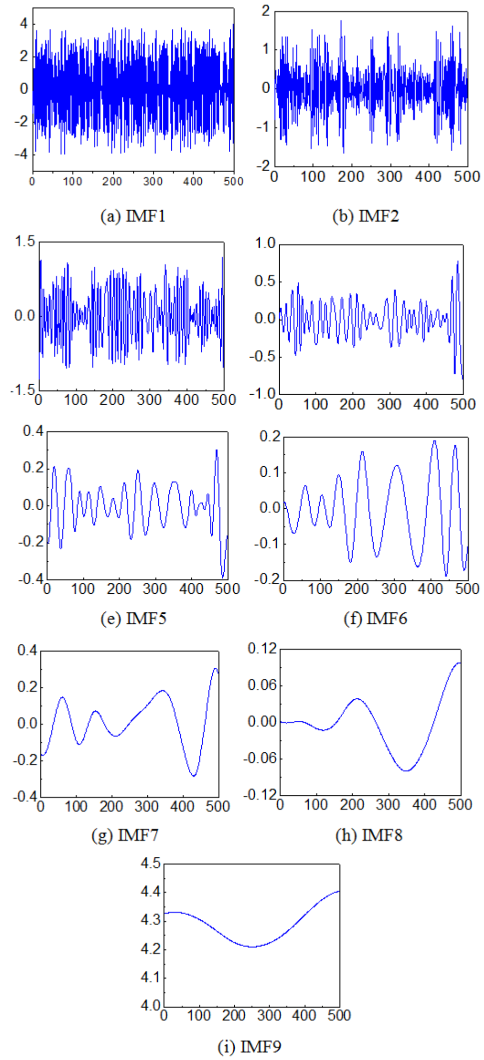

Fig. 3: IMF components of collector's body vibration signals

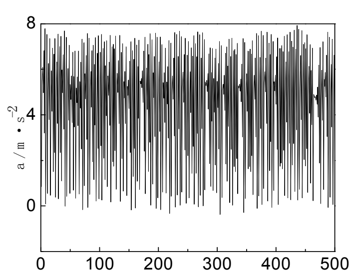

Fig. 4: IMF components' decomposition of caterpillar nodule collector's body vibration signals

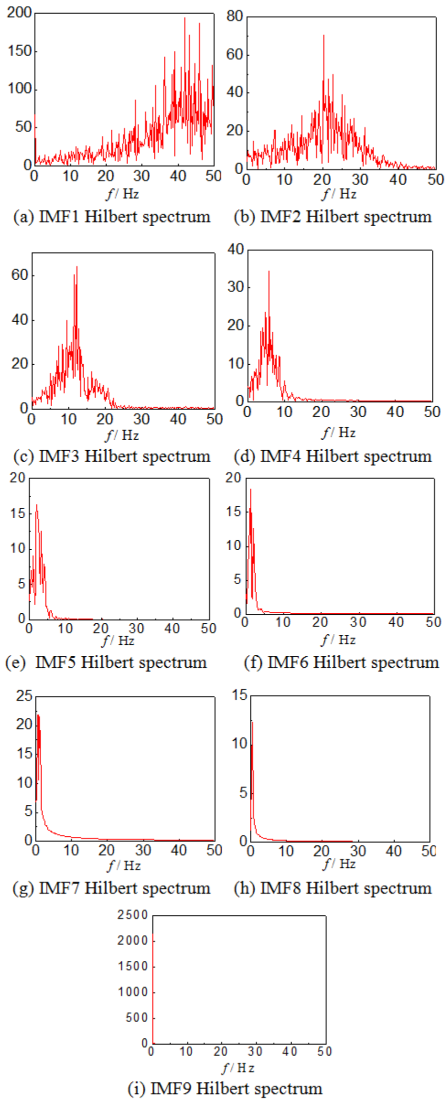

Fig. 5: IMF components' Hilbert spectrum of caterpillar nodule collector's body vibration signals

The outcome of practical test notes that the major cause for the irregular waves of the collector's body vibration signals derives from diverse factors, consisting of wind, wave, current and high pressure of sea bottom etc, while it's running on the soft quality bottom of the sea. So the diesel's body vibration signals with noise are initially implemented EMD decomposition. Judging from the analysis of IMF components' Hilbert spectrum, such as illustrations in Fig. 4, it unveils that the power of collector's vibration signals is intensive on IMF1, IMF2, IMF3, IMF4, IMF9, so that except IMF5, IMF6, IMF7与IMF8, the rest of IMF components are about to be reconstructed for the purpose of getting collector's body vibration signals after denoising according to Fig. 5. The test for the real displacement during the process of collector's body vibration displays the fact that the reconstructed

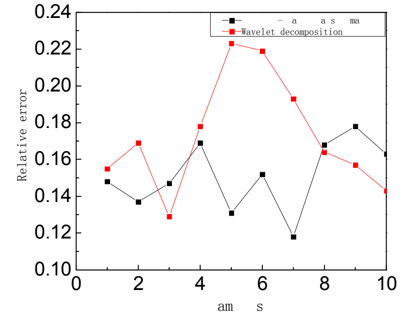

Fig. 6: The relative error of the actual data

signals can simulate the mode of authentic tendency that caterpillar nodule collector's body vibrates when it's walking on the soft quality bottom of the sea.

Comparison between the reconstructed signals and real data: Ten sets of samples are selected and analyzed in order to compare collector's body vibration signals' decomposed and reconstructed wavelet signals with the comparative errors between Hilbert-Huang transformation reconstruction signals and the real data. The comparisons of the errors lie in Fig. 6.

It is evident in Fig. 6 that the relative maximum errors of Hilbert-Huang transformation's reconstructed signals are about 17.8%, relative minimum errors 11.8%, relative medium errors 17.3%. And those for wavelet packet decomposition are 22.3, 14.3 and 17.3%, respectively. It is evident that the relative error of Hilbert-Huang transformation's reconstructed signals is minor to those of wavelet packet's decomposed and reconstructed signals.

CONCLUSION

- EMD approach, by which each IMF component contains local feature information of original signals by self-adapting decomposition based on local feature information, have some physical significance; While adopting the method of decomposing signals by wavelet packet decomposition, wavelet packet's basis function should be determined in advance and wavelet decomposition is not a self-adaptive decomposition approach any more.
- Hilbert-Huang changes and the analysis of wavelet packet's decomposed and reconstructed signals turn out that Hilbert-Huang changes, with the valid reconstructed signals of natural mode can possibly reflect on the essential characteristics of the body vibration signals and figure to improve the control accuracy of driving control system to support caterpillar nodule collector's running on the soft quality bottom of the sea.

ACKNOWLEDGMENT

The study is supported by Hunan Provincial Natural Science Foundation of China (No. 11JJ3059), Industrial support project in Hunan Science and technology (No. 2010GK3091), Excellent Youth Foundation subsidized project of Hunan provincial education department (No. 10B058) and National Natural Science Foundation Project (No. 51105386).

REFERENCES

Alsdorf, N., 1997. Reduction in seismic data using Fourier correlation coefficient filtering [J]. Geophysics, 62(5): 1617-1627.

Chang, C.P. and J.C. Lee, 2009. Using empirical mode decomposition for iris recognition [J]. Comp. Stand. Inter., 31: 729-739.

Dai, Y. and L. Shao-Jun, 2009. Multi-rigid-body modeling and simulation analysis for tracked vehicle [J]. Comput. Simul., 26(3): 281-285. (In Chinese)

Dong, K., S.H. Paek and H.S. Oh, 2008a. A Hibert-Huang transform approach for predicting cyber-attacks [J]. J. Korean Statist. Soc., 37: 277-283.

Dong, Y.F., Y.M. Li and M.K. Xiao, 2008b. Analysis of earthquake ground motions using an improved Hilbert-Huang transform [J]. Soil Dynam. Earthq. Eng., 28: 7-19.

Jia-Qiang, E., W. Chun-Hua and G. Jin-Ke, 2008. Process on measurement data from copper pyrometallurgical heat dynamical system by using of EMD method [J]. Chinese J. Nonferr. Met., 18(5): 946-951 (In Chinese).

Li, X.L., D. Li and Z.H. Liang, 2008. Analysis of depth of anesthesia with Hilbert-Huang spectral entropy [J]. Clin. Neurophysiol., 119: 2465-2475.

Liu, S.J., L. Li and G.G. Wang, 2003. Virtual reality research of ocean poly-metallic nodule mining based on COMRA's mining system [A]. Proceedings of the 5th ISOPE Ocean Mining Symposium [C]. Tsukuba, Japan, pp: 104-117.

Loutridis, S.J., 2004. Damage detection in gear system using empirical mode decomposition [J]. Eng. Struct., 26: 1833-1841.

Rai, V.K. and A.R. Mohanty, 2007. Bearing fault diagnosis using FFT of intrinsic mode functions in Hilbert-Huang transform [J]. Mech. Syst. Signal Proc., 21: 2607-2615.

Wang, Z.Y. and S.J. Liu, 2004. Crawling feasibility simulation study on tracked vehicle for deep ocean mining [J]. J. Syst. Simul., 16(4): 644-646.

Wei, Y.C., C.J. Lee and W.Y. Hung, 2010. Application of Hilbert-Huang transform to characterize soil liquefaction and quay wall seismic responses modeled in centrifuge shaking-tabel tests [J]. Soil Dynam. Earthq. Eng., 30: 614-629.

Xian-Liang, W., J. Dan and W. Liang-Zhi, 1996. A method for singularity extraction from targets transient response with spline functions and rational approximation [J]. J. China Univ., Sci. Technol., 26(4): 528-533 (In Chinese).